Threshold Gain Temperature Dependence of Composite Resonator Vertical-Cavity Lasers

Ann C. Lehman, *Student Member, IEEE,* and Kent D. Choquette, *Fellow, IEEE*

***Abstract*—Vertical-cavity surface-emitting lasers (VCSELs) with two optically coupled but electrically isolated cavities form composite resonator vertical-cavity lasers (CRVCLs). These devices may lase at one of two wavelengths depending on the bias conditions to the two cavities and temperature. A model of the modal gain is presented, which explains the lasing wavelength at threshold based on the spatial and spectral overlap of the microcavity optical modes with the two gain regions.**

***Index Terms*—Coupled-cavity, threshold current, threshold gain, vertical-cavity surface-emitting laser (VCSEL).**

I. Introduction

VERTICAL-CAVITY surface-emitting lasers (VCSELs) have established their place in data communication applications over traditional edge-emitting lasers due in part to their single longitudinal mode output characteristics. One version of a VCSEL is a composite resonator vertical-cavity laser (CRVCL), which is most simply a multicavity VCSEL. The CRVCL discussed here refers to a VCSEL with two electrically isolated but optically coupled active regions separated by a partially transmitting middle mirror. The reflectivity of the middle mirror controls the optical coupling between the cavities, which results in nondegenerate spectral splitting [1].

Because of their unique structures, CRVCLs are being examined for various communication applications. Research has already focused on active/passive devices, in which only one cavity contains a gain region [1]. Some particularly attractive properties of CRVCLs include wavelength switching between two longitudinal modes [2], Q-switching [3], and high single-mode power [4]. Applications include wavelength division multiplexing [5] and optical modulation using polarization switching [6].

Previous research has focused on characterizing the modal properties of CRVCLs [7]. In this paper, the threshold behavior of one cavity with regards to temperature, carrier injection into the secondary cavity, and the resulting output longitudinal mode of a CRVCL are reported and modeled. We show that with one cavity held at a constant current, the threshold current to the other cavity shows a similar threshold dependence on temperature as that of a VCSEL [8]. This behavior is complicated by the existence of two longitudinal modes and can be understood by the spectral and spatial overlap of these modes with the gain in the lasers. The ability to design the threshold current and lasing mode will aid the development of CRVCLs for emerging applications in communication and sensing.

Manuscript received October 12, 2004; revised June 21, 2005.

The authors are with the Department of Electrical and Computer Engineering, University of Illinois at Urbana-Champaign, Urbana, IL 61801 USA.

Digital Object Identifier 10.1109/JSTQE.2005.853851

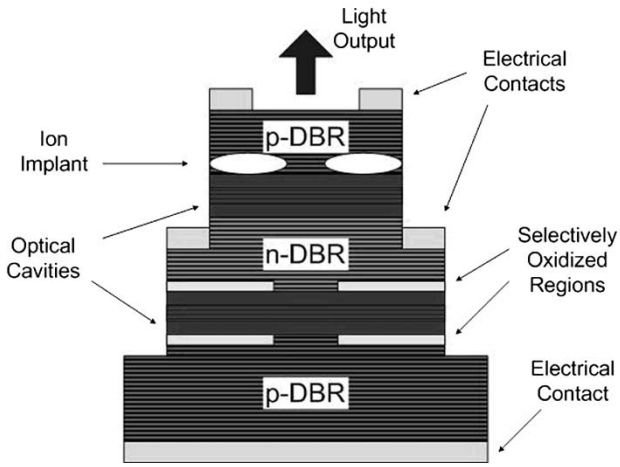

Fig. 1. Structure of CRVCL [7].

II. Experiment

A. Device Description

The devices examined in this paper, shown in Fig. 1, consist of quarter-wave distributed Bragg reflector (DBR) stacks with 35, 10.5, and 21 periods for the bottom, middle, and top mirrors, respectively. Each CRVCL has two active regions that are one wavelength long and contain five GaAs quantum wells producing gain nominally centered at 835 nm. The CRVCL considered in this work has one longitudinal cavity resonance near 860 nm and one near 870 nm. Transverse confinement for the bottom cavity is achieved with an oxide aperture and for the top cavity with ion implantation. The diameters of the implant and oxide apertures are approximately 6 and 12 μm, respectively.

B. Experiment Description

The CRVCLs are probe tested on a temperature-controlled platen under continuous wave operation. The light intensity and spectral characteristics are monitored, and a fiber positioned over the device connected to an optical spectrum analyzer (OSA) is used to determine the lasing resonance. In order to examine the change in threshold characteristics of the CRVCLs caused by varying temperature and bias conditions, a constant current is supplied to the bottom (oxide-confined) cavity while the current to the top (ion implanted) cavity is increased until one of the modes reaches lasing threshold. This is repeated as a function of platen temperature. This procedure is also repeated for a fixed current to the top cavity and a variable current to the bottom cavity.

III. Results

A. Threshold Gain

For a microcavity laser, both spatial and spectral alignment between the gain region and bandwidth with the optical mode resonance must occur. The *spatial overlap* between the optical mode and the active region is determined by the epitaxial design of the VCSEL structure [9]. Through proper placement of the antinode of the longitudinal field, an enhancement of the relative confinement factor can be achieved [10], [11]. In the CRVCL, each longitudinal mode will overlap both active regions, but for each active region the overlap will not be necessarily identical.

The dependence of the threshold current on temperature in VCSELs is well documented [8], [9], [12]–[15]. To summarize, the *spectral overlap* between the gain bandwidth and cavity resonance is the dominant cause of the temperature dependence [8]. For a Fabry–Perot edge-emitting semiconductor laser, many longitudinal modes fall within the gain bandwidth and so the modes closest to the gain peak will lase. Thus, the laser gain essentially selects the lasing mode. Unlike these devices, the short cavity length of a VCSEL results in at most one longitudinal cavity mode spectrally overlapping the gain region. Hence, lasing occurs only at the frequency of the single overlapping cavity resonance. Changing the temperature causes the gain and cavity resonance to shift spectrally but at different rates. More exactly, as temperature increases, the gain peak shifts to longer wavelengths with respect to the cavity resonance. Therefore, the VCSEL threshold current will be approximately lowest at a temperature where the cavity resonance nears spectral alignment with the peak of the gain curve. For temperatures higher and lower than this temperature, the cavity resonance overlaps lower values of gain for the same injection current, and thus increased injection current (higher gain) is required to reach threshold.

The CRVCL's temperature dependence of threshold will be influenced by both the spatial and spectral overlap between gain regions and cavity modes. Because the dual coupled-cavity system is significantly more complex than that of a conventional VCSEL (two gain curves plus two longitudinal modes), it is not immediately clear how the threshold current of CRVCLs will vary with temperature although spectral characterization has been done examining variations of bias conditions [7].

For simplicity, the resonance occurring at the shorter wavelength will be referred to as the short mode, and likewise, the resonance occurring at the longer wavelength will be referred to as the long mode. Each mode is assumed to have a higher amplitude in one cavity than the other as presented in [16] for weakly to moderately-coupled non-frequency-locked cavities. The assumptions for the devices studied here are that the short mode is slightly more dominant in the bottom cavity and that the long mode is slightly more dominant in the top cavity, which will be shown to agree with the data presented.

B. Threshold Measurements

Because confinement and spectral behavior will vary between devices across a sample due, for example, to growth nonuniformities, we focus on two neighboring CRVCLs. If one cavity is driven at a constant current, then the threshold current injected into the other cavity can be measured as a function of temperature. The amount of current in the first cavity affects the total absorption that current injection into the second cavity must overcome before lasing can occur. For threshold current measured in the bottom cavity while the top cavity is not pumped and vice versa, the short mode is always the first to lase below a certain temperature for the devices tested. This implies that the cavity resonances initially occur at longer wavelengths than the peak of the gain curves. Since the gain for both cavities is designed to be peaked at about 835 nm, the assumption that the resonances are at longer wavelengths than the peak of the gain at room temperature is consistent with the measured resonances of 860 and 870 nm. Increasing the temperature of operation will change which of the two cavity resonances overlaps with the highest value of gain and therefore, which mode will reach threshold first. Generally, at lower temperatures the short mode will lase at threshold, and at higher temperatures the long mode will lase at threshold.

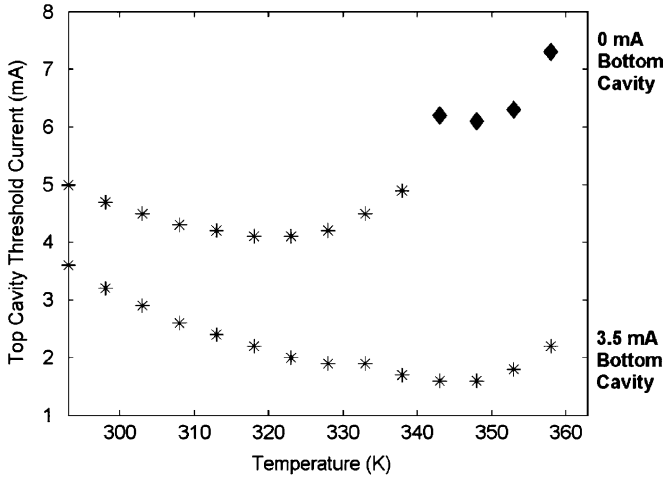

Fig. 2. Threshold current of the top cavity and dominant longitudinal mode for two biases on the bottom cavity is shown. For the upper points, bottom cavity current is 0 mA. For the lower points, bottom cavity current is 3.5 mA. An asterisk indicates that the short mode lased, and a diamond indicates that the long mode lased.

In Fig. 2, the threshold current of the top cavity is measured while the bottom cavity current is set to 0 mA (upper points) and 3.5 mA (lower points). An asterisk indicates that the short mode lased at threshold, and a diamond indicates that the long mode lased at threshold. With 3.5 mA applied to the bottom cavity, the threshold current versus temperature plot is very similar in shape to the case of a VCSEL with the minimum threshold occurring near 70° C. When no current is applied to the bottom cavity, however, the results are notably different. In this case, the threshold minimum occurs around 50° C, and at higher temperatures, the lasing mode switches to the longer wavelength where there is a second apparent relative minimum around 75° C.

Different modal behavior is obtained when the current to the top cavity is held constant and threshold is measured for the

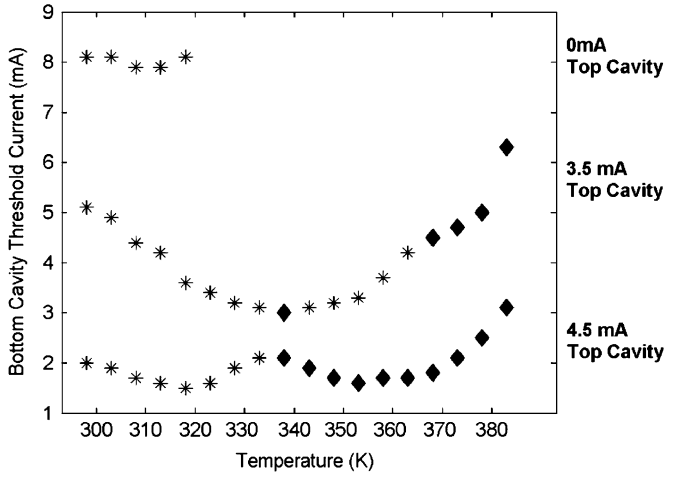

Fig. 3. Threshold current of the bottom cavity and dominant longitudinal mode for various biases on the top cavity. For the upper points, top cavity current is 0 mA. For the middle points, top cavity current is 3.5 mA. For the lower points, top cavity current is 4.5 mA. An asterisk indicates that the short wavelength lased, and a diamond indicates that the long wavelength lased.

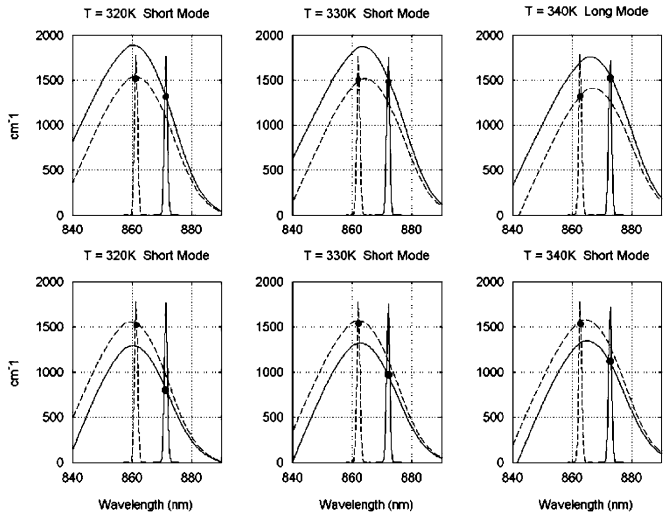

Fig. 4. Plots of effective gain and cavity resonances. The intersection of each cavity resonance with its effective gain curve is marked with a point. The top plots correspond 1.7×10^{12} carriers/cm^{-2} in the bottom cavity, and the bottom plots correspond to 3.7×10^{12} carriers/cm^{-2} in the bottom cavity. The top cavity gain is increased until threshold (1500 cm^{-1}) is met as plotted here. Each column corresponds to a different temperature as labeled.

bottom cavity as shown in Fig. 3 for top cavity biases of 0, 3.5, and 4.5 mA. When the top cavity has no applied bias, the peak gain aligns with the cavity resonance around 35° C, and because the absorption losses are relatively high, the device only lases to temperatures near 55° C. Increasing the top cavity injection to 3.5 mA decreases the injection current needed in the bottom cavity for the threshold condition to be met. It also shifts the minimum threshold current to a higher temperature, which is 65° C. (The lasing of the long mode at the threshold current minimum in Fig. 3 was only observed in a few devices and is disregarded in our analysis.) Increasing the top cavity current to 4.5 mA further decreases threshold current for the bottom cavity, and the temperature at which lasing switches from the short to the long mode at threshold is reduced to 65° C.

C. Threshold Simulation

The data shown in Figs. 2 and 3 can be understood by incorporating an effective modal gain caused by each mode's spatial overlap with both gain regions. This is an extension of the description of effective or modal gain of a laser in which the spatial overlap of the field with the material gain of a single active region is considered [9]

$$\gamma_{\text{eff}} = \Gamma \gamma_{\text{material}} \tag{1}$$

where Γ is a coefficient between zero and one, which reflects the amount of spatial overlap the mode has with the gain region. For the case of two gain regions pumped with different injection currents, (1) can be extended to account for the spatial overlap a mode with the different gain regions in each cavity

$$\gamma_{\text{eff},i} = \Gamma_{\text{top},i} \gamma_{\text{material-top}} + \Gamma_{\text{bottom},i} \gamma_{\text{material-bottom}} \tag{2}$$

where i indicates the long or short wavelength mode, and $\Gamma_{\text{top(bottom)},i}$ gives the fraction of the longitudinal mode overlap of mode i with the top (bottom) cavity's gain region. Because each mode may have a higher amplitude in one cavity than in the other, Γ_{top} and Γ_{bottom} will have different values which reflect this. Due to the relatively large spectral separation between the two longitudinal modes, each may have a different effective gain.

An example for the CRVCL model is shown in Fig. 4. In these calculations, the gain in the bottom cavity is fixed in each row while the top cavity gain is increased until one of the modes reaches threshold, which corresponds to the situation of Fig. 2. The modal threshold gain profiles are then plotted with the cavity resonances which are assumed to shift with temperature at a rate of 0.07 nm/°C [13]. For the top plots, the bottom cavity has a low pumping equivalent to 1.7×10^{12} carriers/cm^3, and for the bottom plots, the bottom cavity has a higher injection current equivalent to 3.7×10^{12} carriers/cm^3. The gain curves have been generated using a free carrier gain model from LaserMod [17]. The calculation is an 8×8 K·P band structure computation to calculate the density of states and solves various semiconductor equations including the Poisson and continuity equations to determine the quasi-Fermi levels as described in [13], [18]–[20]. Because the short mode lases at threshold for low temperatures whether the top cavity or bottom cavity is pumped, the modes may be assumed to overlap both cavities to some degree. The degree of the wavefunction localization is determined from the values of Γ, which we have used as fitting parameters for the simulation of the data. Therefore, the effective gain for the short mode, which is more dominant in the bottom cavity, is found assuming $\Gamma_{\text{top}} = 0.45$ and $\Gamma_{\text{bottom}} = 0.55$ in (2). The effective gain for the long mode, which is more dominant in the top cavity, is found assuming $\Gamma_{\text{top}} = 0.55$ and $\Gamma_{\text{bottom}} = 0.45$ in (2). The solid effective gain curves in Fig. 4 correspond to the effective gain for long mode, and the dotted effective gain curves correspond to the effective gain for the short mode. (The material gain curves for each cavity are not

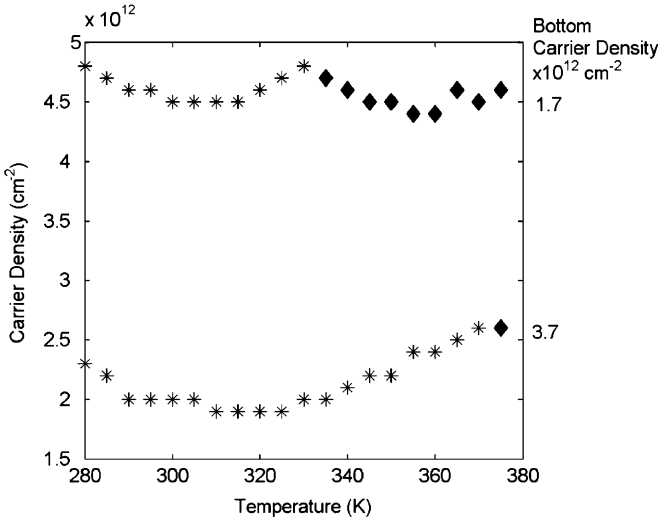

Fig. 5. Modeled threshold carrier density of the top cavity and dominant longitudinal mode for various biases on the bottom cavity. An asterisk indicates that the short wavelength lased, and a diamond indicates that the long wavelength lased. Threshold gain is assumed to be at 1500 cm^{-1}.

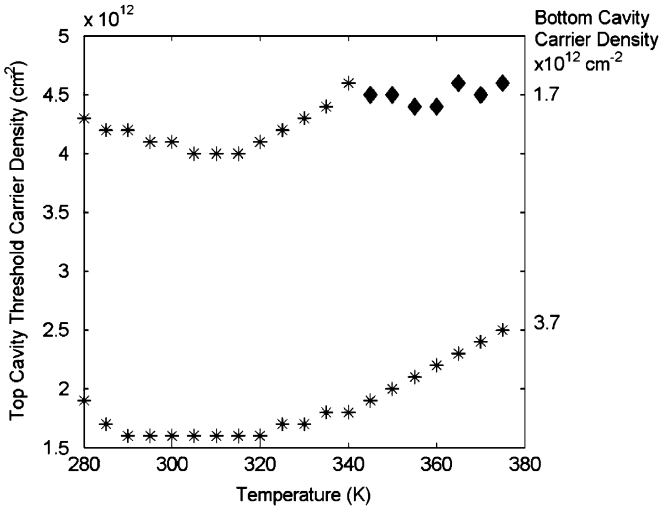

Fig. 6. Modeled threshold carrier density of the top cavity and dominant longitudinal mode for various biases on the bottom cavity. An asterisk indicates that the short wavelength lased, and a diamond indicates that the long wavelength lased. Threshold gain is assumed to be at 1300 cm^{-1} for the short mode and 1500 cm^{-1} for the long mode.

shown.) To determine which mode is lasing at threshold, one must look at where the short mode overlaps the dotted gain curve and where the long mode overlaps the solid gain curve as shown by the points in the plots of Fig. 4. These plots were generated assuming a threshold gain of 1500 cm^{-1} for both modes.

In Fig. 5, the threshold carrier densities and lasing modes are calculated for a series of temperatures. As in Fig. 4, the carrier densities to the bottom cavity are 1.7×10^{12} and 3.7×10^{12} carriers/cm^2 for the two sets of points. This can be compared to the experimental data in Fig. 2. It is clear that the general trends are the same between the two figures. For instance, for low injection to the bottom cavity, there is a threshold minimum of the short mode and at higher temperatures, a threshold minimum of the long mode. For a higher injection to the bottom cavity, the short mode dominates at threshold over a larger temperature range. One notable difference between the two plots is that the minimum threshold densities for low injection into the bottom cavity in Fig. 5 are approximately the same for the long and short modes unlike in Fig. 2 where the local minimum threshold current is lower when the short mode is lasing. For this to occur, each mode must experience a different amount of loss. From the data in Fig. 2, we can determine that the short mode should have less loss. In Fig. 6, we repeat these calculations but assume threshold for the short mode is reduced to 1300 cm^{-1} while threshold for the long mode remains 1500 cm^{-1}. A relatively larger threshold for the long mode is consistent with the formation thermal lens, which is needed to form for optical guiding in the top cavity [9]. Since the long mode overlaps more of the top cavity, it should have a higher threshold gain relative to the short mode.

The longitudinal modal switching in Fig. 3 can be understood with the help of Figs. 7 and 8. In Fig. 7, the top cavity of the CRVCL is being pumped at 3.0×10^{12} and 4.5×10^{12} carriers/cm^2 for the top and bottom rows, respectively, while the bottom cavity injection is increased until threshold is reached

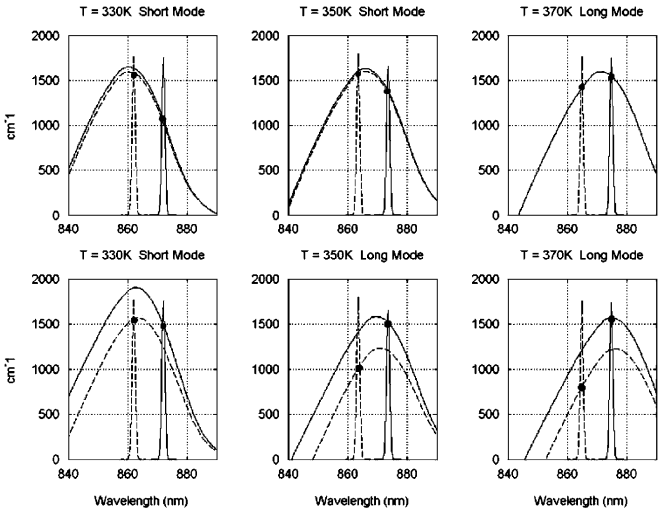

Fig. 7. Plots of effective gain and cavity resonances. The intersection of each cavity resonance with its effective gain curve is marked with a point. The top plots correspond 3.0×10^{12} carriers/cm^{-2} in the top cavity, and the bottom plots correspond to 4.5×10^{12} carriers/cm^{-2} in the top cavity. The bottom cavity gain is increased until threshold (1500 cm^{-1}) is met as plotted here. Each column corresponds to a different temperature as labeled.

for one of the modes. In Fig. 8, the three simulations correspond to top cavity carrier densities of $1.1 \times 10^{12}, 3.0 \times 10^{12}$, and 4.5×10^{12} carriers/cm^2. Once again, the short mode is associated the dotted effective gain curve and asterisks, and the long mode is associated with the solid gain curve and diamonds. For the low applied bias to the top cavity in the top set of points in Fig. 8, the short mode reaches threshold first as carrier injection increases to the bottom cavity for low temperatures but does not have enough gain at the necessary frequency for lasing at higher temperatures. This is consistent with the 0-mA top cavity current experimental data in Fig. 3. When the injection is increased to the top cavity as depicted in the middle row of

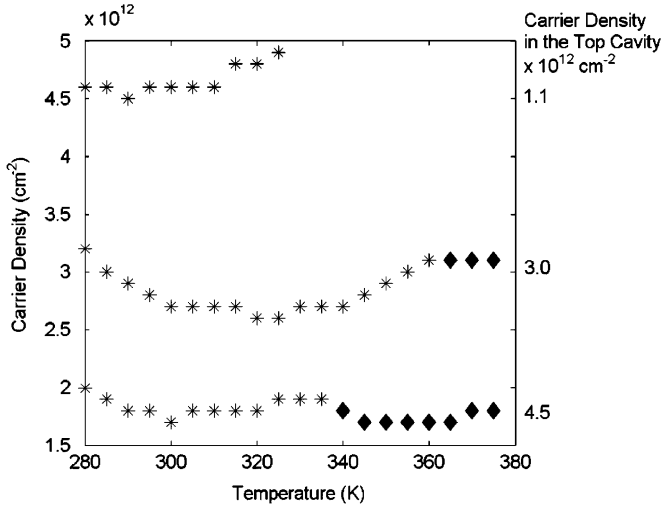

Fig. 8. Modeled threshold carrier density of the top cavity and dominant longitudinal mode for various biases on the bottom cavity. An asterisk indicates that the short wavelength lased, and a diamond indicates that the long wavelength lased. Threshold gain is assumed to be at 1500 cm^{-1}.

points in Fig. 8, the short mode lases at threshold, but the long mode lases first as temperature increases towards 100° C. This is similar to the 3.5-mA top cavity current data in Fig. 3. When injection current is further increased, dominance between the shorter to the longer mode switches at a lower temperature near 65° C corresponding to 4.5-mA top cavity current in Fig. 3 and the bottom set of points in Fig. 8. It is clear that in both the model and experimental data as pumping is increased to the top cavity, the range of temperatures over which the longer wavelength mode will dominate at threshold increases.

A framework describing which mode of a CRVCL will lase at threshold is illustrated in Figs. 4–8. This model takes into account the longitudinal spatial overlap of each cavity resonance with the gain spectrum from both cavities. After accounting for the spatial overlap, the spectral overlap is then analyzed to determine the threshold behavior of the device. Because the loss of each mode in the device is not known, it is difficult to quantitatively apply this model to the experimental results, but it is clear the model correctly reproduces the trends of the experimental data presented in Figs. 2 and 3.

IV. Summary

This work has examined the threshold modal characteristics of CRVCLs under variation of both bias conditions and temperature. In general, CRVCLs have two resonances, which are separated by 10 nm in the devices measured here. The wavefunction of the shorter wavelength mode is found to be predominantly in the bottom cavity whereas the wavefunction of the longer wavelength mode is found to be predominantly in the top cavity. The behavior of the modes was examined by varying the current to one cavity, while current to the other cavity was held constant. In the devices studied here, simultaneous lasing of both modes was not observed.

The threshold behavior of CRVCLs has been modeled by considering both the spatial and spectral overlap between the cavity resonance and gain. The spatial overlap is accounted for with an effective gain curve for each mode. This curve corresponds to the amount each wavefunction of the modes overlaps with the gain in each of the cavities. We estimate the distribution of the wavefunctions to be 45% in one cavity 55% in the other cavity for the devices studied here. The dependence of threshold current on temperature for various biasing conditions of a particular CRVCL is compared to VCSEL behavior. The effective gain theory is found to explain the shape of the threshold versus temperature curves as well as to indicate which mode lases at threshold based on operating temperature and bias conditions. This model can thus be used to understand and predict the threshold behavior of CRVCLS, which will be necessary for optimization of these novel devices for emerging applications.

Acknowledgment

The authors would like to thank K. Geib and A. Allerman at Sandia National Laboratories.

References

[1] A. J. Fischer, K. D. Choquette, W. W. Chow, H. Q. Hou, and K. M. Geib, "Coupled resonator vertical-cavity laser diode," *Appl. Phys. Lett.*, vol. 75, no. 19, pp. 3020–3022, 1999.

[2] R. P. Stanley, R. Houdre, U. Oesterle, M. Ilegems, and C. Weisbuch, "Coupled semiconductor microcavities," *Appl. Phy. Lett.*, vol. 65, no. 16, pp. 2093–2095, 1994.

[3] A. J. Fischer, W. W. Chow, K. D. Choquette, A. A. Allerman, and K. M. Geib, "Q-switched operation of a coupled-resonator vertical-cavity laser diode," *Appl. Phys. Lett.*, vol. 76, no. 15, pp. 1975–1977, 2000.

[4] A. J. Fischer, K. D. Choquette, W. W. Chow, A. A. Allerman, D. K. Serkland, and K. M. Geib, "High single-mode power observed from a couple-resonator vertical-cavity laser diode," *Appl. Phys. Lett.*, vol. 79, no. 25, pp. 4079–4081, 2001.

[5] E. W. Young, D. M. Grasso, A. C. Lehman, and K. D. Choquette, "Dual-channel wavelength-division multiplexing using a composite resonator vertical-cavity laser," *IEEE Photon. Technol. Lett.*, vol. 16, no. 4, pp. 966–968, Apr. 2004.

[6] D. M. Grasso and K. D. Choquette, "Polarization switching in composite-resonator vertical-cavity lasers," *Appl. Phys. Lett.*, vol. 83, no. 25, pp. 5148–5150, 2003.

[7] D. M. Grasso and K. D. Choquette, "Threshold and modal characteristics of composite-resonator vertical-cavity lasers," *IEEE J. Quantum Electron.*, vol. 39, no. 12, pp. 1526–1530, Dec. 2003.

[8] W. W. Chow, S. W. Corzine, D. B. Young, and L. A. Coldren, "Many body effects in the temperatures dependence of threshold in a vertical-cavity surface-emitting laser," *Appl. Phys. Lett.*, vol. 66, no. 19, pp. 2460–2430, 1995.

[9] K. J. Ebeling, "Analysis of vertical cavity surface emitting laser diodes (VCSEL)," in *Semiconductor Quantum Optoelectronics: From Quantum Physics to Smart Devices, Scottish Universities Summer School in Physics*, A. Miller, E. Ebrahimzadeh, and D. M. Finlayson, Eds: St. Andrews, U.K.: Sussp Publications, 1998, vol. 50, pp. 295–338.

[10] M. Y. A. Raja, S. R. J. Brueck, M. Osinski, C. F. Schaus, T. M. Brennan, and B. E. Hammons, "Surface-emitting, multiple quantum well GaAs/AlGaAs laser with wavelength-resonant periodic gain medium," *Appl. Phys. Lett.*, vol. 53, no. 18, pp. 1678–1680, 1988.

[11] S. W. Corzine, R. S. Geels, J. W. Scott, R. H. Yan, and L. A. Coldren, "Design of a Fabry-Perot surface-emitting lasers with a periodic gain structure," *IEEE J. Quantum Electron.*, vol. 25, no. 6, pp. 1513–1524, Jun. 1989.

[12] B. Tell, K. F. Brown-Goebeler, R. E. Leibenguth, and F. M. Baez, "Temperature dependence of GaAs-AlGaAs vertical cavity surface emitting lasers," *Appl. Phys. Lett.*, vol. 60, no. 6, pp. 683–685, 1992.

[13] D. B. Young, J. W. Scott, F. H. Peters, M. G. Peters, M. L. Majewski, B. J. Thibeault, S. W. Corzine, and L. A. Coldren, "Enhanced performance of offset-gain high-barrier vertical-cavity surface-emitting lasers," *IEEE J. Quantum Electron.*, vol. 29, no. 6, pp. 2013–2022, Jun. 1993.

[14] S. Rapp, J. Piprek, K. Streubel, J. Andre, and J. Wallin, "Temperature sensitivity of 1.54-um vertical-cavity lasers with an InP-based bragg reflector," *IEEE J. Quantum Electron.*, vol. 33, no. 10, pp. 1839–1845, Oct. 1997.
[15] H. C. Schneider, A. J. Fischer, W. W. Chow, and J. F. Klem, "Temperature dependence of laser threshold in an InGaAsN vertical-cavity surface-emitting laser," *Appl. Phys. Lett.*, vol. 78, no. 22, pp. 3391–3393, 2001.
[16] W. W. Chow, "Composite resonator mode description of coupled lasers," *IEEE J. Quantum Electron.*, vol. 22, no. 8, pp. 1174–1183, Aug. 1986.
[17] Lasermod Software, RSoft Design Group.
[18] J. J. Dudley, D. L. Crawford, and J. E. Bowers, "Temperature dependence of the properties of DBR mirrors used in surface normal optoelectronic devices," *IEEE Photon. Technol. Lett.*, vol. 4, no. 4, pp. 311–314, Apr. 1992.
[19] F. Oyafuso, P. von Allmen, M. Grupen, and K. Hess, "Inclusion of band-structure and many-body effects in a quantum well laser simulator," *VLSI Des.*, vol. 8, pp. 463–468, 1998.
[20] J. Hader, S. W. Koch, and J. V. Moloney, "Microscopic theory of gain and spontaneous emission in GaInNAs laser material," *Solid-State Electron.*, vol. 47, pp. 513–521, 2003.

Ann C. Lehman (S'04) received the B.S. and M.S. degrees in electrical engineering from the University of Illinois at Urbana-Champaign, Urbana, in 2002 and 2004, respectively. She is currently working toward the Ph.D. degree in electrical engineering at the University of Illinois under Prof. Kent D. Choquette.

Her research interests include the design and fabrication of photonic crystal VCSELs and other optoelectronic devices.

Ms. Lehman is a student member of IEEE-LEOS.

Kent D. Choquette (M'97–SM'02–F'03) received the B.S. degrees in engineering physics and applied mathematics from the University of Colorado, Boulder, in 1984 and the M.S. and Ph.D. degrees in materials science from the University of Wisconsin, Madison, in 1985 and 1990, respectively.

In 1990, he held a postdoctoral appointment at AT&T Bell Laboratories, Murray Hill, NJ. In 1992, he joined Sandia National Laboratories, Albuquerque, NM, as a postdoctoral researcher and in 1993 as a Principal Member of Technical Staff. He became a Professor in the Electrical and Computer Engineering Department, University of Illinois at Urbana-Champaign, Urbana, in 2000. His research group is centered around the design, fabrication, and characterization of vertical-cavity surface emitting lasers (VCSELs), novel microcavity light sources, nanofabrication technologies, and hybrid integration techniques. From 2000 to 2002, he was a IEEE/LEOS Distinguished Lecturer. He has authored over 150 publications and three book chapters, and has presented numerous invited talks and tutorials on VCSELs.

Dr. Choquette is a Fellow of IEEE/LEOS and a Fellow of the Optical Society of America (OSA). He has served as an Associate Editor of the IEEE JOURNAL OF QUANTUM ELECTRONICS, Guest Editor of the IEEE JOURNAL OF SELECTED TOPICS IN QUANTUM ELECTRONICS, and is presently an Associate Editor of the IEEE PHOTONIC TECHNOLOGY LETTERS.